Reliable Renewable Generation and Transmission Expansion Planning: Co-Optimizing System's Resources for Meeting Renewable Targets

Alexandre Moreira, *Student Member, IEEE*, David Pozo, *Member, IEEE*, Alexandre Street, *Member, IEEE*, and Enzo Sauma, *Senior Member, IEEE*

***Abstract*—The current renewable-driven generation expansion wave, pushed by high renewable targets, is not accompanied by the same movement in the transmission expansion planning (TEP) side. In this context, new techniques are needed to balance the cost of relying in expensive reserve resources and the cost of building new lines to ensure least-cost reserve deliverability and foster new renewable projects. The situation is worsened in the presence of contingencies, where the interaction between the optimal reserve siting and deployment, the amount of renewable curtailment, the construction of new lines, and the selection of candidate renewable sites to be developed became even more complex. This paper presents a two-stage min-max-min model for co-optimizing the expansion of the transmission system and renewable generation capacity to meet renewable targets under high security standards and renewable uncertainty. In order to account for realistic reserve needs and its interaction with the expansion plan, correlations between renewables injection as well as generation and transmission (GT) outages are accounted for in a robust fashion. In order to ensure security within a flexible framework, the concept of compound GT $n-K$ security criteria is presented. Three case studies are proposed to illustrate the applicability of the proposed model. A case study with realistic data from the Chilean system is presented and solutions obtained with different levels of security are tested against a set of 10 000 simulated scenarios of renewable injections and system component outages.**

***Index Terms*—Generation and transmission security criterion, renewable generation and transmission expansion planning, renewable targets, reserve deliverability and siting, wind curtailment.**

Manuscript received June 7, 2016; revised October 21, 2016; accepted November 12, 2016. Date of publication November 22, 2016; date of current version June 16, 2017. This work was supported in part by CNPq under Grant 307030/2014-8 and under the *Science without Borders* scholarship program under Grant 203274/2014-8; in part by CAPES - Atração de Jovens Talentos under Grant 88881.030337/2013-01, project number 88887.124362/2014-00; in part by CONICYT, FONDECYT/Regular under Grant 1161112; and in part by CONICYT, PCI/REDES under Grant 150008. Paper no. TPWRS-00867-2016.

A. Moreira (CNPq Scholarship Student — Brazil) is with the Department of Electrical and Electronic Engineering, Imperial College London, London SW7 2AZ, U.K. (e-mail: a.moreira14@imperial.ac.uk).

D. Pozo was with the Department of Industrial and Systems Engineering, Pontificia Universidad Católica de Chile, Santiago 7630614, Chile. He is now with the Department of Electrical Engineering, Pontifical Catholic University of Rio de Janeiro, Rio de Janeiro 22430-060, Brazil (e-mail: davidpozocamara@gmail.com).

A. Street is with the Department of Electrical Engineering, Pontifical Catholic University of Rio de Janeiro, Rio de Janeiro 22430-060, Brazil (e-mail: street@ele.puc-rio.br).

E. Sauma is with the Department of Industrial and Systems Engineering, Pontificia Universidad Católica de Chile, Santiago 7630614, Chile (e-mail: esauma@ing.puc.cl).

Color versions of one or more of the figures in this paper are available online at http://ieeexplore.ieee.org.

Digital Object Identifier 10.1109/TPWRS.2016.2631450

NOMENCLATURE

The mathematical symbols used throughout this paper are classified below as follows.

Sets

I	Set of generator indexes.
I_b	Set of indexes of generators connected to bus b.
$\mathcal{L}^C$	Set of indexes of candidate transmission lines.
$\mathcal{L}^E$	Set of indexes of existing transmission lines.
$\mathcal{L}$	Set of indexes of all transmission lines, equal to $\left(\mathcal{L}^E \cup \mathcal{L}^C\right)$.
N^E	Set of indexes of existing buses.
N^{RE}	Set of indexes of candidate buses with potential renewable energy.
N	Set of indexes of buses, equal to $\left(N^E \cup N^{RE}\right)$.

Parameters

Γ^D	Conservativeness parameter.
Γ^W	Conservativeness parameter.
Σ^D	Estimated nodal demand covariance matrix.
Σ^W	Estimated nodal renewable generation covariance matrix.
$\overline{\Delta D}_{K,\Sigma}$	Maximum level of system power imbalance for an $n-K$ security criterion.
C_l^{Cap}	Cost per MW of candidate lines.
C^{RE}	Construction cost of new node with potential renewable energy.
C_K^I	Cost of imbalance under the worst-case contingency having K contingencies.
C_l	Construction cost of candidate line l.
C_i^p	Production cost of generator i.
C_i^d	Reserve-down cost of generator i.
C_i^u	Reserve-up cost of generator i.
$\hat{D}_b$	Nominal demand at bus b.
$\overline{F}_l^{Min}$	Minimum power flow capacity of candidate line l.
$\overline{F}_l^{Max}$	Maximum power flow capacity of candidate line l.
$\overline{F}_l$	Power flow capacity of existing line l.
$fr(l)$	Sending or origin bus of line l.
K	Number of unavailable system components.
$\boldsymbol{L}^D$	Lower triangular matrix that satisfies the equality $\boldsymbol{\Sigma}^D = \boldsymbol{L}^D \boldsymbol{L}^{DT}$.

$\boldsymbol{L}^W$ Lower triangular matrix that satisfies the equality $\boldsymbol{\Sigma}^W = \boldsymbol{L}^W \boldsymbol{L}^{W\,T}$.
n Number of system components.
$\overline{P}_i$ Capacity of generator i.
R_i^D Reserve-down limit of generator i.
R_i^U Reserve-up limit of generator i.
$to(l)$ Receiving or destination bus of line l.
$Target$ Target of renewable generation as percentage of the total demand.
$\hat{W}_b$ Expected renewable generation at bus b.
x_l Reactance of line l.

Decision Variables

$\Delta D_b^{+\,\mathrm{wc}}$ Power surplus equivalent to the energy spillage at bus b under the worst-case contingency.
$\Delta D_b^{-\,\mathrm{wc}}$ Power deficit equivalent to the energy insufficiency at bus b under the worst-case contingency.
$\Delta D_{K,\Sigma}$ Worst-case system power imbalance, given K and first-level decisions.
θ_b Phase angle at bus b in the pre-contingency state.
θ_b^{wc} Phase angle at bus b under the worst-case contingency.
a_i^G Binary variable that is equal to 0 if generator i is unavailable under the worst-case contingency, being 1 otherwise.
a_l^L Binary variable that is equal to 0 if line l is unavailable under the worst-case contingency, being 1 otherwise.
D_b Demand at bus b.
$\mathbf{e}^d$ Error on the demand.
$\mathbf{e}^w$ Error on the renewable generation.
$\overline{F}_l^C$ Power flow capacity of line l.
f_l Power flow of line l in the pre-contingency state.
f_l^{wc} Power flow of line l under the worst-case contingency.
p_i Power output of generator i in the pre-contingency state.
p_i^{wc} Power output of generator i under the worst-case contingency.
v_l Binary variable that is equal to 1 if candidate line l is built, being 0 otherwise.
W_b Renewable generation at bus b.
y_b Binary variable that is equal to 1 if candidate bus b is built, being 0 otherwise.

I. Introduction

AIMING to reduce greenhouse gases emissions, power systems worldwide are utilizing more energy from renewable sources. To this end, setting renewable targets is one of the mechanisms largely adopted to guide this process with tight levels of renewable penetration. Many countries have established policy targets related to renewable energy. The European Union (EU), for example, established a target to meet 20% of its energy consumption by means of renewable sources by 2020 [1]. Some EU member countries have more strict targets, e.g., Germany with 30% by 2020 and 60% by 2050. To address the variability of such resources under tight security criteria, the system might require additional levels of quick-response reserves to circumvent contingencies under the uncertainty of intermittent injections of the renewable sources. Within this framework, the transmission system plays a key role, allowing the system operator to use the cheapest resources to ensure system reliability. However, transmission systems were not designed to cope with such levels of renewable penetration. Therefore, a renewable-driven expansion of the generation demands a reorientation of current electricity networks. Several technical reports and scientific articles have highlighted the importance of transmission investments to achieve renewable energy targets [2]–[4].

Transmission expansion planning (TEP) has typically been addressed by a reactive approach, where the transmission planner reacts by building transmission lines to interconnect committed generation expansion projects. However, a proactive approach for TEP has recently captured the attention of researchers and Regulatory Authorities as an alternative to the reactive approach. In the proactive approach, the transmission planner anticipates the best generation investment decisions. In this manner, the transmission planner is able to induce generation expansions with higher social welfare. Several works have shown the benefits of using a proactive TEP instead of a reactive TEP (see [5]–[7]). Proactive transmission planning is a type of co-optimization that is particularly relevant for large transmission investments to connect remote areas with high renewable generation potential with load demands. The recognition of co-optimization for transmission and generation capacity expansion has been reported in several works and technical reports [2]–[5], [8]. In the specific case of renewables, where candidate areas are, in general, known in advance and aggressive incentive (subsides) policies are largely used to drive new investments, the co-optimization of the transmission system and the new capacity of renewable generation is a powerful tool for planners, police makers, and regulators. Within this framework, it is possible to efficiently achieve high renewable penetration targets [3] while accounting for the complex interaction between the selection of new renewable sites and candidate transmission lines.

In addition to that, the proper determination of reserve levels and siting for a reliable operation of power systems under the presence of large amounts of renewable energy sources is a timely topic. Several works [9]–[12] have suggested that reserve needs and costs increase when renewable penetration rises. Clearly, the expansion of renewable projects changes the manner of operating power systems, and therefore, significantly impacts the optimal transmission plan and the optimal reserve sitting. Furthermore, renewable energy resources are usually located in remote areas, distant from load-demand centers and conventional generation (reserves). Such characteristics of renewable sources generally impact the capability of the system to guarantee *reserve deliverability*, whose importance has been highlighted in [13] and [14]. On the other side, investments in intermittent renewable projects, such as wind farms, can be financially jeopardized by renewable curtailment. In order to address wind curtailment in the operational side, system operators make use of system's resources [15]. Hence, the side effect of curtailing renewable resources could be mitigated by means of the joint optimization of system's resources in the planning level.

The situation of curtailing renewable resources and/or shedding load is worsened in the presence of contingencies. In nowadays, worldwide Regulatory Authorities are including $(n-1)$ security criterion as common standard of reliability. However, some of them are moving for higher reliability standards. This is the case of North American Electric Reliability Corporation (NERC) [16] that requires a contingency analysis to consider the loss of two elements simultaneously or consecutively.

Two-stage robust optimization [17], also known as adjustable robust optimization (ARO), has been extensively utilized for operation problems with large renewable penetration [18]–[20]. This approach is also emerging in transmission planning applications with renewable energy generation [21]. A large number of robust models have been proposed in the literature considering reserve deliverability in the operation framework. For instance, [20] explicitly considers the cost of reserve scheduling and deliverability by means of joint energy and reserve scheduling. In the planning literature however, recent publications in two-stage robust optimization models (see [22], [23]) aiming to address renewable variability and security criteria in TEP problems are proposed based on single-period static models. While in [22] renewable variability and generation contingencies are considered by means of demand and generation capacity uncertainty, disregarding transmission line failures, in [23] generation and line outages are accounted for, disregarding the effect of renewable variability.

Therefore, the objective of this work is to propose a two-stage renewable generation and transmission expansion planning (RG-TEP) model that jointly finds the best subset of new transmission assets and renewable sites to be developed. The main goal of this co-optimization planning model is to address renewable targets while accounting for the least-cost reserve scheduling to ensure reserve deliverability under generation and transmission outages and renewable variability.

To meet the objective and goal of the proposed model, the cost of optimal reserve levels allocated throughout the expanded network is also considered. This allows for balancing the cost of relying in expensive reserve resources, possibly incurring in significant amounts of penalties for curtailing renewable resources, and the cost of building new lines to ensure least-cost reserve deliverability and minimal renewable curtailment. In order to account for realistic reserve needs and its interaction with the expansion plan, correlations between renewables injection as well as generation and transmission outages are accounted for in a worst-case fashion. In order to ensure security within a flexible framework, the concept of compound GT $n-K$ security criteria is presented. Within the proposed security criteria, the uncertain renewable generation and demand must be addressed with different user-defined thresholds for the maximum allowed system power imbalance. Thus, it is possible to plan the expansion of the system in order to simultaneously guarantee 0% of system power imbalance for security criteria, $n-0$ and $n-1$, while permitting, e.g., a maximum of 1% and 2.5% of system power imbalance for, respectively, $n-2$ and $n-3$ security criteria. Such modeling feature extends previous works ([12], [22]–[24]) while providing more flexibility and constitutes a highly practical feature for system planners.

In summary, the main contributions of this paper are the following:

1) Formulating a novel two-stage min-max-min static RG-TEP model for co-optimizing transmission and renewable generation capacity expansion to meet renewable targets under correlated uncertainty for renewable injections and equipment failures.
2) Accounting for reserve deliverability through the expanded network by explicitly modeling the cost of the optimal siting and deployment under the presence of different security criteria and correlated renewable generation. It is worth emphasizing that under such new features, the trade-off between building more lines to ensure cheaper reserve deliverability and reduce renewable curtailment or relying in existing reserve resources is implicitly embedded in the optimal plan.
3) Expanding the notion of uncertainty sets in the framework of robust optimization for power systems planning by considering two sets of uncertainties, not simultaneously covered in the state of the art literature: (a) lines and generating units outages and (b) correlated renewable generation (and loads) through the Cholesky decomposition of the covariance matrix. It is worth mentioning that the solutions obtained are tested against out-of-sample simulated scenarios to corroborate the effectiveness of the worst-case modeling choice.
4) Introducing the concept of compound (combined) GT $n-K$ security criteria in transmission expansion planning in which the level of imbalance under line and generation contingency events (independent or not) can be controlled in the planning stage for different user-defined levels of severity.

As a consequence of the aforementioned contributions, the proposed model provides planners with an effective computational planning methodology capable of assessing the trade-off between additional security criteria in a very flexible fashion based on industry standards ($n-K$ criteria) and the cost of operating and expanding the system under different levels of renewable penetration and correlation patterns.

The remainder of the paper is organized as follows. Section II describes the mathematical model formulation for the TEP problem and Section III presents the solution methodology used to solve the problem. In Section IV, the new modeling features and the proposed solution approach are illustrated with case studies. Finally, the study's conclusions are presented in Section V.

II. Mathematical Formulation

The proposed RG-TEP model aims at determining the optimal renewable generation and transmission expansion plan considering correlated nodal injection uncertainty as well as multiple security criteria while ensuring reserve deliverability. A conventional method to address this problem would be a single-level formulation that exhaustively and explicitly enumerates all possible cases of contingencies for all the comprised multiple security criteria combined with several possible scenarios of renewable generation realization. This, in fact, is a highly

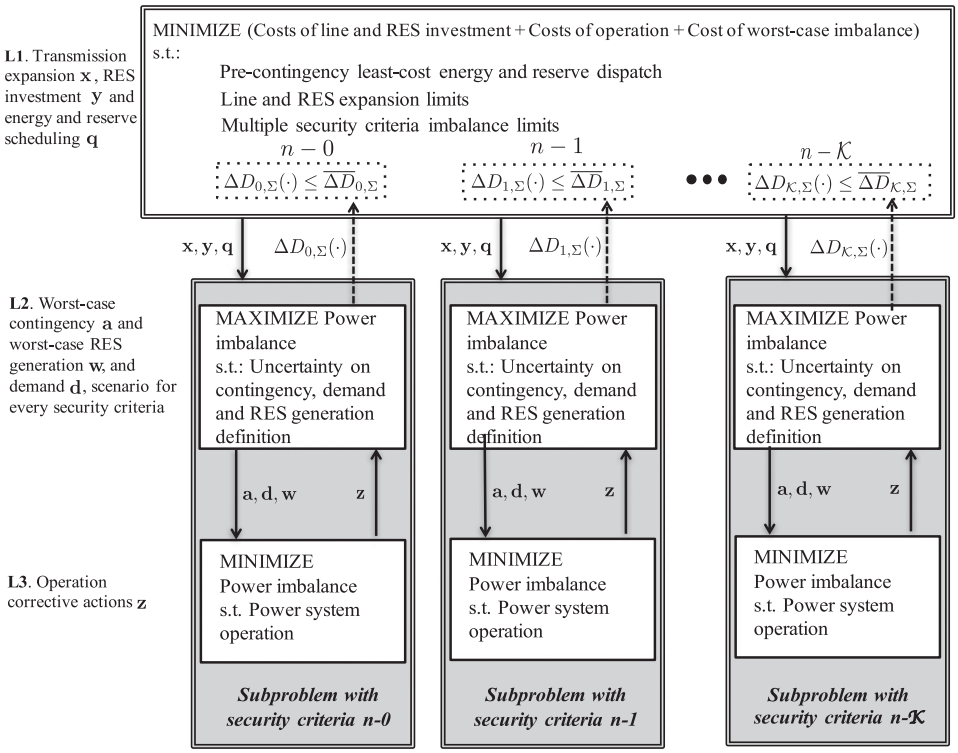

Fig. 1. Three-level robust TEP framework.

combinatorial problem that can easily become intractable,[1] e.g. see [23].

In this paper, we not only consider individual security criteria, but also multiple security criteria simultaneously along with nodal injection uncertainty. In this case, it is necessary to decompose the problem in different levels. In this context, we present an adaptive robust optimization model to address the aforementioned objectives that leads to a trilevel problem. Then, the two lowermost optimization problems represent an oracle that finds the worst-case scenario, i.e., a single scenario that causes the most severe imbalance in the system. This oracle replaces the very large bunch of constraints added to the RG-TEP problem mimicking all future operations for each scenario.

Each level, as illustrated in Fig. 1, has its role described below.

1) *First Level*: This problem determines the investment plan, i.e., it decides which candidate buses with potential renewable generation, $\mathbf{y}$, should be built and which candidate lines should be installed and how much should be their capacities, $\mathbf{x}$. In addition, pre-contingency energy and reserve system dispatch, $\mathbf{q}$, is also determined by the first level while meeting constraints associated with power balance, power flow, and generation limits.
2) *Second Level*: Given the first-level decisions on investments and operation, the second level seeks to identify the contingency as well as the renewable nodal injection and load demand realization that would together lead to the worst-case system power imbalance. If the imposed security criterion is $n-1$, the contingency state identified in the second level will comprise the worst-case failure of one of the system elements. If it is $n-2$ instead, the contingency identified will comprise the worst case combination of failures of two system elements. The same rationale applies for any $n-K$ security criterion. Hence, the second level finds simultaneously the values for the uncertainty parameters of renewable generation $\mathbf{w}$, load demand $\mathbf{d}$, and element failures $\mathbf{a}$, that generate the worst imbalance in the system.
3) *Third Level*: Once first and second level decisions are taken, the third level determines the post-contingency corrective actions, $\mathbf{z}$, to circumvent the worst-case realization of renewable generation and outages of system elements imposed in the second level. These corrective actions are performed by making use of the resources provided by the first level decision, e.g., newly built lines and scheduled reserves.

Note that, as we comprise multiple security criteria simultaneously in our formulation, second and third levels are replicated for each considered security criterion (see Fig. 1). For example, for the compound security criterion $K(0 \rightarrow 1)$, we have replicated second and third level problems for each individual security level, namely $n-0$ (where only renewable uncertainty is considered) and $n-1$ (where both renewable and $n-1$ security criterion are considered).

Before describing the full formulation of the problem, we introduce some detailed definition for uncertain parameters of renewable generation, load demand and elements outages. The

[1]In [23] for comparison purposes, a conventional single-level formulation to address a TEP problem considering individual security criteria was implemented. Due to computational limitations, when the imposed security criterion was tighter than $n-1$, such model could not be solved to optimality for the 118-bus system with 311 elements (number of generators plus the number of existing and candidate transmission lines). For $n-3$, it was not even possible to load the matrix of the problem into the computer memory.

mathematical symbols used throughout this paper are summarized in the nomenclature section.

A. Renewable Generation, Demand and Elements Availability Uncertainties

Each contingency state is represented by a binary-decision vector, $\mathbf{a} = [\mathbf{a}^G|\mathbf{a}^L]$, whose components indicate the availability of each element, e.g., a_i^G represents the availability of the generating unit i, i.e., it has the value of 1 if generator i is available and 0 otherwise. Similarly, a_l^L is related to the availability of transmission line l. Similarly to [20], spatial correlation between nodal demands and between nodal renewable injections can be accounted for in the two-stage robust modeling framework by their nodal covariance matrices ($\mathbf{\Sigma}^d, \mathbf{\Sigma}^w$), which are factorized via Cholesky decomposition [25], i.e, $\mathbf{\Sigma}^d = \mathbf{L}^d(\mathbf{L}^d)^\top$ for demand and $\mathbf{\Sigma}^w = \mathbf{L}^w(\mathbf{L}^w)^\top$ for RES generation. In this work, we propose the consideration of both types of uncertainty factors through the following contingency-dependent renewable generation and demand polyhedral uncertainty set:

$$\mathcal{U}_{\Sigma,K}^{\mathbf{a},\mathbf{d},\mathbf{w}} = \left\{ (\mathbf{a},\mathbf{d},\mathbf{w}) \in \{0,1\}^n \times \mathbb{R}^{n^d \times n^w} \;\middle|\; \sum_i a_i^G + \sum_l a_l^L \geq n - K \right.$$
$$\mathbf{d} = \hat{\mathbf{d}} + s^d \mathbf{L}^d \mathbf{e}^d, \| \mathbf{e}^d \|_1 \leq \Gamma^d, \mathbf{e}^d \in [-1,1]^{n^d}$$
$$\left. \mathbf{w} = \hat{\mathbf{w}} + s^w \mathbf{L}^w \mathbf{e}^w, \| \mathbf{e}^w \|_1 \leq \Gamma^w, \quad \mathbf{e}^w \in [-1,1]^{n^w} \right\}. \quad (1)$$

In (1), $\mathbf{e}^d$ and $\mathbf{e}^w$ define normalized error vectors whose components assume values between -1 and 1 for all n^d-demand-variable nodes and n^w-RES nodes, $\hat{\mathbf{d}}$ and $\hat{\mathbf{w}}$ are the vectors of nominal values of demand and RES generation, respectively, and $(\mathbf{d}, \mathbf{w})$ is the scenario realization of the nodal-demand and RES generation for a given pair of error vectors. The uncertainty budget, represented by Γ^d and Γ^w for demand and RES generation, respectively, controls the number of uncertain parameters that can deviate from their nominal value by means of norm-1 constraints imposed to the error vectors. Additionally, the amplitudes of such deviations are controlled by s^d and s^w, respectively. Therefore, in the proposed uncertainty set, the level of conservativeness or stress associated with the renewable injection and demand is controlled by those four parameters, whereas the conservativeness associated with contingencies is controlled by the parameter K. It is relevant to say that, although possible cross-correlation between loads and renewable injections could be easily accounted for in the proposed framework, for the sake of simplicity, we do not consider it in this work. Furthermore, it is important to emphasize the modeling flexibility in this framework. For instance, two or more different uncertainty sets with the same security level can be used to model regional-security criteria or to skip some of the contingencies chosen by the user while still keeping the system reliable under variable demand and renewable generation injection. In the next section, we take advantage of this modeling flexibility to introduce the concept of a *compound GT $n-K$ security criterion* under the presence of correlated demand and renewable injections.

B. The Reliable RG-TEP Model

Following the modeling framework of previous reported work on static planning [21]–[23], the complete three-level problem is formulated accordingly:

$$\min_{\substack{\Delta D_{K,\Sigma},\theta_b,\overline{F}_l^C,\\ f_l,p_i,r_i^d,r_i^u,v_l,y_l}} \left\{ \sum_{i\in I} C_i^P p_i + \sum_{i\in I} C_i^d r_i^d + \sum_{i\in I} C_i^u r_i^u + \sum_{l\in\mathcal{L}^C} \left(C_l v_l + C_l^{Cap} \overline{F}_l^C \right) + \sum_{b\in N^{RE}} C_b^{RE} y_b + \sum_{K\in\mathcal{K}} C_K^I \Delta D_{K,\Sigma} \right\} \quad (2)$$

subject to:

$$\sum_{i\in I_b} p_i + \sum_{l\in\mathcal{L}|to(l)=b} f_l - \sum_{l\in\mathcal{L}|fr(l)=b} f_l = \hat{D}_b - \hat{W}_b; \quad \forall b \in N^E \quad (3)$$

$$\sum_{i\in I_b} p_i + \sum_{l\in\mathcal{L}|to(l)=b} f_l - \sum_{l\in\mathcal{L}|fr(l)=b} f_l = -y_b \hat{W}_b; \quad \forall b \in N^{RE} \quad (4)$$

$$\sum_{b\in N^{RE}} y_b \hat{W}_b + \sum_{b\in N^E} \hat{W}_b \geq Target \sum_{b\in N^E} \hat{D}_b \quad (5)$$

$$f_l = \frac{1}{x_l}\left(\theta_{fr(l)} - \theta_{to(l)}\right); \forall l \in \mathcal{L}^E \quad (6)$$

$$-M_l\left(1-v_l\right) \leq f_l - \frac{1}{x_l}\left(\theta_{fr(l)} - \theta_{to(l)}\right) \leq M_l\left(1-v_l\right); \forall l \in \mathcal{L}^C \quad (7)$$

$$-\overline{F}_l \leq f_l \leq \overline{F}_l; \forall l \in \mathcal{L}^E \quad (8)$$

$$-\overline{F}_l^C \leq f_l \leq \overline{F}_l^C; \forall l \in \mathcal{L}^C \quad (9)$$

$$v_l \overline{F}_l^{Min} \leq \overline{F}_l^C \leq v_l \overline{F}_l^{Max}; \forall l \in \mathcal{L}^C \quad (10)$$

$$\sum_{l\in\mathcal{L}^C|to(l)=b} v_l + \sum_{l\in\mathcal{L}^C|fr(l)=b} v_l \leq y_b M_b^o; \forall b \in N^{RE} \quad (11)$$

$$0 \leq p_i \leq \overline{P}_i; \forall i \in I \quad (12)$$

$$p_i + r_i^u \leq \overline{P}_i; \forall i \in I \quad (13)$$

$$p_i - r_i^d \geq 0; \forall i \in I \quad (14)$$

$$0 \leq r_i^u \leq R_i^U; \forall i \in I \quad (15)$$

$$0 \leq r_i^d \leq R_i^D; \forall i \in I \quad (16)$$

$$v_l \in \{0,1\}; \forall l \in \mathcal{L}^C \quad (17)$$

$$y_b \in \{0,1\}; \forall b \in N^{RE} \quad (18)$$

$$\Delta D_{K,\Sigma} \leq \overline{\Delta D}_{K,\Sigma}, \forall K \in \mathcal{K} \quad (19)$$

$$\Delta D_{K,\Sigma} = \max_{(\mathbf{a},\mathbf{d},\mathbf{w})\in\mathcal{U}^{\mathbf{a},\mathbf{d},\mathbf{w}}_{\Sigma,K}} \min_{\substack{\Delta D_b^{+\mathrm{wc}},\Delta D_b^{-\mathrm{wc}},\\ \theta_b^{\mathrm{wc}},f_l^{\mathrm{wc}},p_i^{\mathrm{wc}}}} \left\{ \sum_{b\in N} \Delta D_b^{-\mathrm{wc}} + \sum_{b\in N/N^W} \Delta D_b^{+\mathrm{wc}} + \gamma^{Spil} \sum_{b\in N^W} \Delta D_b^{+\mathrm{wc}} \right\} \quad (20)$$

subject to:

$$\sum_{i\in I_b} p_i^{\mathrm{wc}} + \sum_{l\in\mathcal{L}|to(l)=b} f_l^{\mathrm{wc}} - \sum_{l\in\mathcal{L}|fr(l)=b} f_l^{\mathrm{wc}} - \Delta D_b^{+\mathrm{wc}} + \Delta D_b^{-\mathrm{wc}} = D_b - W_b : (\beta_b); \forall b \in N^E \quad (21)$$

$$\sum_{i\in I_b} p_i^{\mathrm{wc}} + \sum_{l\in\mathcal{L}|to(l)=b} f_l^{\mathrm{wc}} - \sum_{l\in\mathcal{L}|fr(l)=b} f_l^{\mathrm{wc}} - \Delta D_b^{+\mathrm{wc}} + \Delta D_b^{-\mathrm{wc}} = -y_b W_b : (\beta_b); \forall b \in N^{RE} \quad (22)$$

$$-M_l(1-a_l^L) \le f_l^{\mathrm{wc}} - \frac{1}{x_l}\left(\theta_{fr(l)}^{\mathrm{wc}} - \theta_{to(l)}^{\mathrm{wc}}\right) \le M_l(1-a_l^L) : (\omega_l,\psi_l); \forall l \in \mathcal{L}^E \quad (23)$$

$$-M_l(1-v_l a_l^L) \le f_l^{\mathrm{wc}} - \frac{1}{x_l}\left(\theta_{fr(l)}^{\mathrm{wc}} - \theta_{to(l)}^{\mathrm{wc}}\right) \le M_l(1-v_l a_l^L) : (\pi_l,\sigma_l); \forall l \in \mathcal{L}^C \quad (24)$$

$$-a_l^L \overline{F}_l \le f_l^{\mathrm{wc}} \le a_l^L \overline{F}_l : (\xi_l,\phi_l); \forall l \in \mathcal{L}^E \quad (25)$$

$$-a_l^L \overline{F}_l^C \le f_l^{\mathrm{wc}} \le a_l^L \overline{F}_l^C : (\gamma_l,\chi_l); \forall l \in \mathcal{L}^C \quad (26)$$

$$a_i^G\left(p_i - r_i^d\right) \le p_i^{\mathrm{wc}} \le a_i^G\left(p_i + r_i^u\right) : (\zeta_i,\lambda_i); \forall i \in I \quad (27)$$

$$0 \le p_i^{\mathrm{wc}} \le \overline{P}_i : (\mu_i); \forall i \in I \quad (28)$$

$$\Delta D_b^{+\mathrm{wc}}, \Delta D_b^{-\mathrm{wc}} \ge 0; \forall b \in N. \quad (29)$$

The objective function, (2), minimizes the following cost-related terms: (i) generation in the pre-contingency, nominal, scenario (where p_i is the generation of each unit i in the set of units I); (ii) up and down reserves (given by the r_i^u and r_i^d decision variables); (iii) line investment (which is given by v_l, a binary variable that defines whether there is investment in a given candidate line l or not, and by $\overline{F}_l^C$ which is a continuous variable that defines the installed capacity of line l); (iv) RES expansion (where y_b is a binary variable that indicates whether a new bus, with a new renewable source, is connected to the system or not); and (v) the system power imbalance for all security criteria comprised in the analysis (where $\Delta D_{K,\Sigma}$ expresses the power imbalance under the worst-case scenario of renewable injection, load, and loss of up to K elements).

Generation costs are calculated via linear cost functions. Up and down reserves costs are associated with reserves scheduled to ensure that the system will be able to meet the demand under the outage of any combination of up to K elements, any demand scenario, and any RES generation realization within a pre-defined uncertainty set. Investment in transmission lines has two terms. The first one is related to the fixed cost of building the line (C^l), and the second one refers to the cost proportional to the line capacity (C^{Cap}). RES-related cost accounts for the incentives that are diminished from society as subsides for driving RES investments and siting. The last term is the worst-case system power imbalance (RES spillage, power surplus, and loss of load) cost associated with the security criterion adopted by the transmission planner.

Constraints (3) and (4) represent the nodal power balance. Constraint (4) refers to the new candidate RES nodes. Note that demand and RES generation are fixed to their nominal values for this pre-contingency problem. Constraint (5) imposes a minimum amount of RES sharing in the demand supply defined by the parameter $Target$, which can be set to a value between 0 and 1. Constraints (6) and (7) model the DC power flow approach to describe the line flows in terms of nodal voltage angles for existing and candidates lines, respectively. Binary variable v_l takes a value of 1 if the line is built and is 0 otherwise. The parameter M_l is a large-enough constant. Constraints (8) and (9) establish power flow capacity limits for existing and candidate lines, respectively. Constraint (10) enforces the line capacity of a candidate line to be 0 if the line is not constructed or to be between some minimum and maximum line capacity bounds, otherwise. To avoid network loops where new RES nodes are built without RES investment, we have included the logic constraint (11). Thus, it is not possible to invest in lines that connect a new RES node if there is no RES investment.

Regarding variable constraints for the first-level problem, the power generation is limited in (12). Up-spinning reserve must be less than the power capacity left in each generating unit in (13). Down-spinning reserve cannot exceed the scheduled power generation in (14). Additionally, maximum up and down spinning reserves are limited for each generating unit based on their technological constraints in (15) and (16). The binary nature of the line and RES investment variables is ensured in (17) and (18). Finally, in (19), the system power imbalance for the worst-case scenario is limited to be less then or equal to a certain user-defined threshold. The worst-case imbalance is an outcome, a value of the objective function, of the two lowermost optimization levels (20)–(29).

In (20), while the outer maximization, the second-level problem, seeks the worst-case scenario of contingency, renewable injection, and load within the uncertainty set (given by expression (1)), the inner objective function, the third-level problem, reproduces the operative reaction for a scenario of load and renewable injection in a given post-contingency state. Therefore, the third level minimizes the total system power imbalance, which is defined here as the weighted sum of load shedding, power surplus, and wind spillage. This problem can be observed as a phase-one problem that aims to ensure second-stage feasibility by minimizing artificial variables that account for constraint violations. In this model, artificial variables related to RES spillage are weighted by a factor γ^{Spil} that relates RES spillage costs with load shedding to make them comparable. Note that N^W is the set of buses containing wind generation, which is composed by both existing and candidate buses.

In (21)–(29), the system operator reaction, redispatch for the worst-case (wc) renewable injection, load scenario, and post-contingency state is accounted for. To differentiate

post-contingency variables from the nominal one set in the first-level problem, variables receive the wc superscript in the third-level. Constraints (21) and (22) relate with the power balance, considering the positive and negative imbalance for existing nodes and new RES candidate nodes, respectively. Power flow definition constraints are given in (23) for the existing lines and (24) for candidate lines. Power flow limits are described in (25) and (26) for existing and candidates lines, respectively. Constraint (27) sets power generation considering the pre-contingency scheduled energy and reserve. Generation limits are set in (28). Non-negative nodal power imbalance variables are depicted in (29). Finally, dual variables associated with each constraint are presented within parenthesis.

III. Solution Approach

The proposed reliable RG-TEP problem formulation, (2)–(29), belongs to the class of trilevel optimization models with multiple recourse functions, [24], which can be solved by a column-and-constraint generation algorithm. To make use of such method, one needs an oracle that identifies the worst-case scenario of load, renewable injection, and contingency for each K and first-level decision. By means of such an oracle, also known as a slave problem or simply a subproblem, the method relies on a master problem, a relaxed version of the extensive form of the trilevel problem where all scenarios and post-contingency states are explicitly considered and is iteratively enhanced with redispatch constraints for the identified worst-case scenarios and post-contingency state.

Although the two lowermost levels, (20)–(29), are conceived to provide precisely the oracle information, such formulation belongs to the class of mixed integer bilevel programming problems. Nevertheless, the bilevel problem (20)–(29) can be conveniently recast as an equivalent single-level program, as performed in [20], [23]. To carry out this transformation, the following steps are needed: 1) the original second-level maximization problem, given by the outer max operator in (20), is rewritten to maximize the third-level dual-objective function; 2) dual feasibility constraints associated with the third-level problem are imposed in the new equivalent model to ensure a lower bound for the optimal value of the third-level problem by means of its dual objective function; 3) bilinear terms associated with products between binary variables of the second-level problem (line and generation contingency variables, a_i^G and a_l^L) and dual variables of the third-level problem are linearized by means of disjunctive constraints, as performed in [23]; and 4) bilinear terms associated with products between third-level dual variables and second-level continuous variables (related to renewable injection and load scenarios) are linearized by means of the binary expansion approach, as performed in [20].[2] Consequently, a mixed integer linear programming (MILP) formulation for the two lowermost levels, hereafter referred to as the oracle, is available and suitable for commercial MILP solvers [27]. For the sake of brevity, we omit the oracle formulation.

Since the master problem relies on a subset of the scenarios in $\mathcal{U}_{\Sigma,K}^{\mathbf{a},\mathbf{d},\mathbf{w}}$, its objective function provides a lower bound for the optimal value of the trilevel problem [23]. Such lower bound can be found by means of the following model in each iteration j of the algorithm:

$$LB^{(j)} = \min_{\substack{\Delta D_{K,\Sigma},\theta_b,\overline{F}_l^C,\\ f_l,p_i,r_i^d,r_i^u,v_l,y_l}} \left\{ \sum_{i\in I} C_i^P p_i + \sum_{i\in I} C_i^d r_i^d + \sum_{i\in I} C_i^u r_i^u + \sum_{l\in\mathcal{L}^C} \left(C_l v_l + C_l^{Cap}\overline{F}_l^C\right) + \sum_{b\in N^{RE}} C_b^{RE} y_b + \sum_{K\in\mathcal{K}} C_K^I \alpha_K \right\} \tag{30}$$

s.t.

$$\text{Constraint (3)–(19)} \tag{31}$$

$$\alpha_K \le \overline{\Delta D}_{K,\Sigma}, \forall K \in \mathcal{K} \tag{32}$$

$$\alpha_K \ge \sum_{b\in N} \Delta D_b^{-\mathrm{wc}(K,m)} + \sum_{b\in N/N^W} \Delta D_b^{+\mathrm{wc}(K,m)} + \gamma^{Spil} \sum_{b\in N^W} \Delta D_b^{+\mathrm{wc}(K,m)}, \forall K \in \mathcal{K}, m = 1,...,j \tag{33}$$

$$\text{Constraint (21)–(29)}^{(K,m)}, \forall K \in \mathcal{K}, m = 1,...,j. \tag{34}$$

In (30)–(34), additional operative variables with the superscript (K,m), namely $f_l^{wc(K,m)}, p_i^{wc(K,m)}, \Delta D_b^{+\mathrm{wc}(K,m)}$ and $\Delta D_b^{-\mathrm{wc}(K,m)}$, are associated with each scenario of the uncertain parameters identified by the oracle for each K at iteration m, namely $\mathbf{d}^{(K,m)}, \mathbf{w}^{(K,m)}$ and $\mathbf{a}^{(K,m)}$. In (30) and (32), the worst-case imbalance function of each criterion is replaced by an auxiliary variable α_K. In (33), such variable is limited from below by the imbalance of each scenario identified in previous iterations. Finally, in (34), (21)–(29) accompanied by the superscript (K,m) indicates that the redispatch constraints (21)–(29) are repeated for each K and iteration m considering different sets of variables identified by the same superscript (K,m).

The upper bound, $UB^{(j)}$, can be found at any iteration j by means of the evaluation of the true objective function, (2), on a trial solution, $\mathbf{x}^{*(j)}$, whose components are all the first-level decision variables $(f_l, p_i, r_i^u, r_i^d, v_l, y_b)$ found by the master problem at iteration j. To do that, the oracle is used to assess the imbalance for each criterion K. In this framework, according to (34), new redispatch variables (columns) and constraints are iteratively included in the master problem until convergence of the algorithm is achieved. Next, we present the column-and-constraint generation algorithm to solve the reliable RG-TEP for large renewable penetration.

[2]It is relevant to say that the uncorrelated case, extensively explored in the recent literature ([19], [21], [26], just to mention a few), fits in the proposed model by considering $\mathbf{\Sigma}^d$ and $\mathbf{\Sigma}^w$ as identity matrices. In this case, the worst-case scenario is always composed by Γ^d and Γ^w components of the nodal demand and nodal-renewable injection vectors, respectively, on the boundaries of the box constraints. Hence, the error variables can be expressed by binary variables and the subsequent bilinear terms associated with those variables linearized according to step 3.

Algorithm 1: Column-and-constraint generation algorithm.

1: Initialize: $j \leftarrow 0$, $UB^{(j)} \leftarrow +\infty$, $LB^{(j)} \leftarrow 0$
2: **if** $\left(UB^{(j)} - LB^{(j)}\right)/UB^{(j)} \leq \epsilon$ **then** STOP
3: **end if**
4: Update the iterations counter: $j \leftarrow j + 1$.
5: Solve the master problem (30)–(34) and store the lower bound, $LB^{(j)}$, and its optimal solution, $\mathbf{x}^{*(j)}$
6: Solve the oracle for each $K \in \mathcal{K}$, fixing the first-level variables to the optimal solution found by the master problem, $\mathbf{x}^{*(j)}$, and store the imbalance $\Delta D_{K,\Sigma}$.
7: Compute $UB^{(j)}$ and go to step 2.

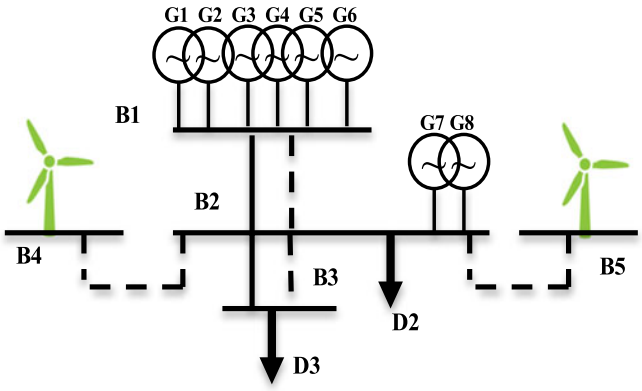

Fig. 2. 3(existing)+2(candidate)-nodes power system.

IV. Case Studies

The performance of the proposed model and solution methodology is illustrated in this section. Three cases are used: the first comprises a small 3(existing)+2(candidate)-bus test system that illustrates the impact of considering multiple security criteria under the presence of correlated-renewable injection uncertainty, the second, based on the main Chilean power system, demonstrates the effectiveness of the proposed methodology in a realistic case study, and the third, based on the standard IEEE 118-bus system, analyses the performance of the solution algorithm for a meshed topology with more than hundred buses. The presented methodology was implemented on a computer with two Intel Xeon E5–2697 v2 processors at 2.7 GHz and 512 GB of RAM, using Xpress-MP 7.8 under MOSEL [27].

A. (3e+2c)-Bus System Case Study

As depicted in Fig. 2, this system has three existing buses with eight conventional generation units and two candidate buses with potential wind generation. The system comprises two existing transmission assets and twenty-one candidates, which are represented by the dashed lines. Each dashed line corresponds to several candidate circuits. In this case study, we set the standard deviation of the renewable generation of buses 4 and 5 to 23.11% of their maximum output and we consider s^w equal to 1. Then, we perform a sensitivity analysis on the correlation factor ρ. The dashed line between buses 1 and 2 comprises 9 candidate circuits, whereas each dashed line between buses 2 and 3, 4 and 2, and 5 and 2 refers to 4 candidate circuits. Detailed data for this case study can be found in the data document [28].

TABLE I
Total Reserve Cost ($/hour)

Correlation	Security Criteria $K(0)$	$K(0 \rightarrow 1)$	$K(0 \rightarrow 2)$	$K(0 \rightarrow 3)$
−100%	0.00	162.00	349.00	1069.22
−50%	95.99	282.19	492.79	6992.92
0%	111.38	300.88	515.38	7945.11
50%	177.50	384.60	654.30	11336.40
100%	248.50	480.50	3693.50	14845.60

TABLE II
Total Investment in Lines ($/hour)

Correlation	Security Criteria $K(0)$	$K(0 \rightarrow 1)$	$K(0 \rightarrow 2)$	$K(0 \rightarrow 3)$
−100%	6704.62	13760.30	21477.00	29307.80
−50%	7916.44	15064.90	22652.90	28361.10
0%	7954.40	15122.20	22791.30	28043.30
50%	7990.86	15159.90	22859.90	29151.10
100%	9319.00	16374.50	22947.00	29330.40

To depict the impact of considering multiple security criteria under the presence of correlated-renewable injection uncertainty, four different combined security criteria are considered in each study: 1) pure $(n-0)$, where only renewable variability is addressed, 2) combined $(n-0)$ and $(n-1)$, 3) combined $(n-0)$, $(n-1)$, and $(n-2)$, and 4) combined $(n-0), (n-1)$, $(n-2)$ and $(n-3)$. Hereinafter, we use the the acronym $K(0)$ to represent a single $(n-0)$ security criterion, whereas $K(0 \rightarrow 3)$ refers to a compound security criterion ranging from $(n-0)$ to $(n-3)$. For all of the composed criteria, renewable variability is considered as described in the previous section. For simplicity purposes, demand variability is neglected.

In this case study, a sensitivity analysis is performed to investigate the impact of correlation between renewable sources under combined security criteria on spinning reserve costs and transmission expansion investments. For the individual security criteria $(n-0)$, $(n-1)$, and $(n-2)$ comprised in the aforementioned combined criteria, we consider the penalization cost $C^I_{K=0,1,2}$ equal to 4×10^3\$/MWh, and for the individual $(n-3)$, the penalization $C^I_{K=3}$ is set to 600\$/MWh. The tolerance for convergence is 5×10^{-3}. In addition, the renewable nominal generation available in the two candidate buses corresponds to 63.1% of the total energy demand. Finally, the spillage factor γ^{Spil} is set to 10^{-2}.

In Table I, the costs associated with reserve levels for each considered correlation and combined security criteria are shown. There is a clear pattern of increase in reserve needs when the security criterion becomes tighter. In addition, as correlation increases, the required levels of spinning reserves become higher.

Table II displays the investments on transmission lines undertaken for each correlation and combined security criteria. As we can see, a correlation increase leads to higher investments in transmission lines for combined security criteria up to $K(0 \rightarrow 2)$. Two reasons are behind this effect. The first is because additional line capacity is needed for the positively correlated peaks of renewable injection. The second relates to reserve deliverability: the higher the correlation between RES buses, the higher the required reserve level to ensure system reliability. Because the cheapest conventional generators are located at bus 1, as long as the correlation grows, more investment is needed to bring cheap reserves from bus 1, i.e., an extra investment is needed to ensure reserve deliverability. However, for the $K(0 \rightarrow 3)$ criterion, the pattern for investments in lines is broken because the candidate lines available are not sufficient to bring cheap reserves from bus 1. This is reflected in the faster rate of growth of reserve costs for $K(0 \rightarrow 3)$ from correlation equal to –100% up to correlation equal to 100%, as reported in Table I.

B. Main Chilean Power System Case Study

We illustrate the proposed model using a stylized representation of the main Chilean power system (Sistema Interconectado Central, or its acronym SIC). The stylized SIC comprises 27 nodes, 52 existing lines, and 282 generating units. The data (transmission lines, generating units, locations, demands, etc.) is obtained from the Chilean Regulatory Authority [29] and SIC System Operator [30]. We have chosen 66 candidates lines for expansion. Full generation, lines and demand data are available in [28]. Our study focuses on the year 2025, for which Chilean Law has set a 20% renewable energy generation target. Nodal demand is projected according to the CNE's technical report [29]. We have considered here that renewable generation targets are reached with wind and solar energy resources only. Potential future RES generation data are obtained from the MAPS-Chile initiative project [31].

We have imposed simultaneous security criteria with different thresholds. System power imbalance is limited in terms of the total demand, to 0% for the individual security criteria $(n-0)$, $(n-1)$, and $(n-2)$ and to 2.5% for the individual $(n-3)$. In addition, load shedding is penalized with a cost of 4×10^4 \$/MWh, and the convergence gap is set to 5×10^{-3} for imbalances from security criteria up to two outages, while imbalances associated with three outages are penalized by 40 \$/MWh, with a convergence gap of 3×10^{-2}. Finally, the penalty factor for renewable curtailment is set to 10^{-3} in this case study.

The model outcomes are summarized in Table III. In columns 2 to 5, results for different security criteria are provided. In rows 1 to 4, we present the costs related to operation of and investment in new transmission lines and renewable energy capacity expansion in thousands of dollars.[3] As it is expected, operation costs increase while the imposed security criteria becomes tighter. However, investment costs in new RES nodes as well as RES penetration remain equal for all security criteria, as shown in rows 4 and 8. In order to accomplish identical RES penetration with different and more stringent security criteria, it is necessary to undertake higher investments in transmission lines. Thus, for the case of planning without security criteria, the number of constructed lines is 14, with a cost of 6.69 thousand of dollars, while for the case of planning the network with $K(0 \rightarrow 3)$ security criteria, the number of built lines increases to 27, resulting in a cost of more than 11 thousand of dollars. It is worth remarking that costs presented in Table III refer to one hour of operation. Thus, the value of 6.69 thousand dollars per hour associated with line investments for $K(0)$ is actually equivalent to approximately 58.60 million dollars per year. Assuming a 30 years life time, this is equivalent to 1.80 billion dollars. Similar results have been reported previously in [32] for the Chilean system. Up- and down-spinning reserves are shown in rows 5 and 6. The levels of up and down reserves rise from light to rigorous security criteria.

TABLE III
RESULTS FOR THE CHILEAN POWER SYSTEM

Security Criteria	$K(0)$	$K(0 \rightarrow 1)$	$K(0 \rightarrow 2)$	$K(0 \rightarrow 3)$
Total Sys. Cost(10^3 \$)	236.89	250.70	261.96	268.79
Total Ope. Cost(10^3 \$)	201.41	215.12	222.72	228.98
Inv. in Trans. Lines(10^3 \$)	6.69	6.77	10.43	11.00
Inv. in New Buses(10^3 \$)	28.80	28.80	28.80	28.80
Down Spinning Reserve(MW)	0	1511.88	2932.13	3035.17
Up Spinning Reserve(MW)	114.00	1161.91	1526.06	2287.67
No. of Lines Built	14	14	25	27
RES Penetration (%)	20.25	20.25	20.25	20.25
Aver. Inv.&Ope. Cost(\$/MWh)	20.94	22.16	23.16	23.76
WC LOL for K = 0 (%)	–	–	–	–
WC LOL for K = 1 (%)	12.16	–	–	–
WC LOL for K = 2 (%)	20.48	5.56	–	–
WC LOL for K = 3 (%)	23.76	13.29	7.82	1.82
Time of resolution (s)	88.01	1408.28	47226.90	78358.40

The optimal number of lines to build, the percentage of renewable penetration, and the total average cost per MWh of demand for each security criterion are respectively shown in rows 7, 8, and 9 of Table III. Note that the average cost of the energy supply is calculated by taking into account operational, RES capacity, and transmission expansion costs. In this study, for a renewable penetration equal to 20.25% of the demand share, for all cases, the average cost slightly increases as the imposed security criteria become tighter. It should be noted that increasing the security level from pure $K(0)$ to $K(0 \rightarrow 1)$ slightly increases investment costs in new lines. In this case, most of the increase in reliability is addressed by significantly higher levels of allocated reserves. However, by moving towards a $K(0 \rightarrow 2)$ criterion to accommodate a RES generation integration in 2025, both the investment plan and reserve levels notably differ from the $K(0 \rightarrow 1)$ case due to the quasi-radial characteristics of the Chilean power system. Nevertheless, since more lines are built for $K(0 \rightarrow 3)$ than for $K(0)$ and these lines are strategically chosen to guarantee security at minimum cost, the delivery of

[3]These results are associated with a single time interval, i.e., a representative worst-case hour obtained by the two lowermost optimization problem. This is consistent with previous reported work on the subject of static planning, [21]–[23], and sufficient to capture the effect of the new features proposed in this study.

TABLE IV
OUT-OF-SAMPLE MONTE CARLO SIMULATION TEST FOR THE CHILEAN POWER SYSTEM

Security Criteria	$K(0)$	$K(0 \rightarrow 1)$	$K(0 \rightarrow 2)$	$K(0 \rightarrow 3)$
LOL Interval	LOL Probability			
$=0\%$	11.77%	85.72%	93.72%	96.88%
(0–1]%	7.65%	2.94%	2.22%	0.87%
(1–2]%	15.99%	4.35%	1.92%	1.10%
(2–3]%	15.44%	2.94%	1.10%	0.60%
(3–4]%	13.84%	1.86%	0.56%	0.24%
(4–5]%	10.25%	1.12%	0.23%	0.19%
(5–10]%	21.81%	1.04%	0.25%	0.12%
$>10\%$	3.25%	0.03%	0.00%	0.00%
Expected LOL	3.49%	0.34%	0.12%	0.06%
CVaR of the LOL	11.13%	4.20%	2.16%	1.23%
Expected Total Costs [10^3\$]	410.01	268.82	269.19	272.46
CVaR of the Total Costs [10^3\$]	746.52	442.48	361.11	330.38

cheaper reserves is facilitated. As a consequence, the operational cost only increases less than 14% from $K(0)$ to $K(0 \rightarrow 3)$, although the up-spinning reserve requirements rise from 114 MW for $K(0)$ to 2287.67 MW for $K(0 \rightarrow 3)$. This reinforces the importance of considering reserve deliverability while planning system expansion as it is proposed in the methodology presented in this paper. The worst-case load shedding for contingencies with up to 3 outages is shown in rows 10 to 13. We observe that planning new RES generation capacity and network expansion without considering any security criteria could lead to cases of severe load shedding costs, 12.16% of the load demand may be caused by a single outage, while up to 23.76% of the load demand can be curtailed by a combination of 3 simultaneous outages. However, by increasing security, the worst-case load shedding drops under the given threshold at the expense of having higher system operational and investment costs, as expected. Finally, CPU times of resolution are shown in row 14.

In order to assess the robustness of the solutions provided by the proposed methodology, we performed an out-of-sample Monte Carlo simulation test aiming to analyze the reliability and cost for the solutions obtained using different compound security criteria. To do that, after running the model, we generated 10000 scenarios assuming independently generated Bernoulli trials for each line and generator state (1 for on-service and 0 for out-of-service state), with 0.1% and 1% probability for the out-of-service states, respectively, according to [33]. Renewable generation output scenarios are obtained by means of multivariate Gaussian random samples with mean equal to the estimated values for the nominal outputs and covariance matrix used in the uncertainty set definition. Table IV shows the load shedding level, or loss of load (LOL), for different solutions, each of them obtained for different security criteria. The expected value (average among all the 10000 scenarios) and the conditional value at risk (CVaR) with 95% confidence (average among the highest 500 scenarios) for the LOL are shown in rows 9 and 10 of Table IV.

In the $K(0)$ case, where no security criterion is enforced and only renewable variability is accounted for through (1) (column 2 of Table IV), there is a high chance of observing a deep LOL. As we can see in this column, the chance of an event in which a LOL of 5 to 10% of the overall system demand takes place exceeds 20%. The 95%-CVaR reaches the amount of 11.13% of the demand although the expected LOL is 3.49% for this case. Thus, by adding up one level of security, $K(0 \rightarrow 1)$ security criterion, the reliability of the system significantly increases. The probability of having zero LOL increases from 11.77% to 85.72% (row 1 of Table IV). However, the total probability of the scenarios with LOL higher than 2% of the demand still surpasses 6%. Therefore, by analyzing the reliability measures for the next two security criteria, the compound $K(0 \rightarrow 2)$ and $K(0 \rightarrow 3)$, it is possible to see satisfactory levels of expected value and 95%-CVaR for the LOL, below 2.16% and 1.23% of the system demand. Also, according to the fourth and fifth columns of Table IV, the probability of experiencing scenarios in which the loss of load is higher than 2% of the system demand falls to 2.2% and 1.1%, respectively.

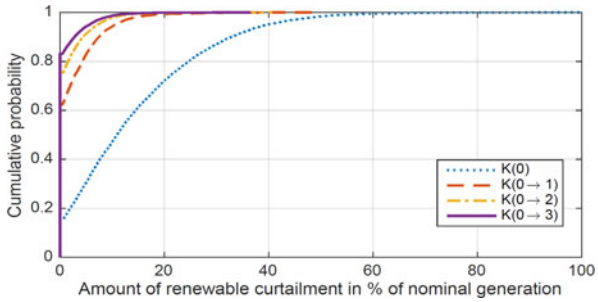

Fig. 3. Empirical CDF of renewable curtailment from Monte Carlo simulation.

The last two rows of Table IV show the expected and 95%-CVaR total (first and second stage) costs for the four planning solutions associated with the security levels. Observe that, as a result of the protection provided by the consideration of more stringent security criteria, the CVaR of the total costs (transmission investments plus operation costs plus system power imbalance costs) decreases with the level of security criterion. Observe that non-considering any security criteria for the transmission planning would result into a more expensive solution due to the high load shedding and renewable curtailment. Fig. 3 shows the cumulative distribution function for the renewable curtailment in terms of percentage of the total demand. Although all optimal expansion plans reach 20.25% of renewable penetration (see Table III), the renewable curtailment significantly decreases with tight security criteria requirement. As consequence, better signals and environment for renewable investors is created. This should be relevant for regulators who aim at targets of renewable penetrations with private investors. The proposed co-optimization of system's resources, which jointly defines new renewable generation, transmission capacity, and new reserve levels and sitting proposed in here allows to tune system reliability by imposing tight security criteria without increasing significantly total costs (see last two rows of Table IV).

C. (118e+4c)-Bus System Case Study

In this case study, we apply the proposed methodology for a modified version of the standard IEEE 118-bus test system.

TABLE V
RESULTS FOR THE (118E + 4C)-BUS SYSTEM

Security Criteria	$K(0)$	$K(0 \rightarrow 1)$	$K(0 \rightarrow 2)$	$K(0 \rightarrow 3)$
Total System Cost(10^3 \$)	18.93	21.72	36.86	37.50
Down Spinning Reserve (MW)	12.00	28.00	28.00	29.00
Up Spinning Reserve (MW)	28.00	301.02	245.28	275.29
Number of Lines Built	6	8	21	21
Time of resolution (s)	14.09	898.76	18,934.50	20,393.70

Here, we consider this system with 118 existing buses, 4 candidates buses with potential renewable generation sources, and 53 candidate transmission lines. Such candidate sources, if connected to the system, can contribute together to meet up to 24.81% of the system demand with their nominal output. Each of these potential renewable sites is considered to have a standard deviation equivalent to 17% of its maximum generation production output. In addition, the correlation factor between the outputs of candidate buses 119 and 120 and between the outputs of candidate buses 121 and 122 are set to 0.75. For the $(n-0)$, $(n-1)$, and the $(n-2)$ security criteria, null load shedding is imposed, whereas, 3.5% of load shedding is allowed in the worst case of triple contingencies. In this case study, the target to meet at least 20% of demand by renewable generation is also imposed. Full data for this case study can be accessed in [28].

Table V summarizes the attained results for this system. Total (operation and investments) system cost increases with the stringency of the security criterion. The renewable generation expansion solution reaches the maximum level (24.81%) available for all criteria. The level of down-spinning reserves grows with the safety of the system. However, the required level of up-spinning reserves decreases from the $K(0 \rightarrow 1)$ to the $K(0 \rightarrow 2)$ security criteria since there is a major investment on the transmission network. This enables the procurement of cheaper reserves to meet the security requirement. This optimal balance between reserves and transmission expansion is only possible due to the explicit consideration of reserves into the RG-TEP problem. Time of resolution is shown in the last row for all criteria. It is lower than the Chilean case study despite that we are considering a larger system in terms of number of buses.

V. CONCLUSION

In this paper, we proposed a RG-TEP model to support the efficient achievement of RES share targets while considering the reliability of the system by accounting for the interaction between reserve deliverability and the network plan. Backed up by our studies, we claim that the growth of the renewable penetration in a power system should be coordinated with the transmission expansion planning to properly accommodate renewable generators and possibly reduce operational costs without compromising the security of the system. A two-stage min-max-min optimization model has been formulated to take into account contingencies as well as uncertainty in demand and renewable generation. The resulting model has been solved using a column-and-constraint generation algorithm. Simulation results presented for the Chilean case study corroborates the effectiveness of the proposed methodology to find robust solutions and its capability to provide system planners with a flexible tool to measure the trade-off between reliability and cost under reasonable computational effort. The methodology is also tested with the standard IEEE 118-bus system in order to demonstrate its scalability.

Finally, further extensions with more focus on multiperiod modeling, flexibilities as corrective transmission switching actions and use of phase shifters or incorporating a dynamic investment framework should be relevant for future research.

ACKNOWLEDGMENT

The authors would like to thank FICO (Xpress-MP developer) for the academic partnership program with the Electrical Engineering Department of the Pontifical Catholic University of Rio de Janeiro (PUC-Rio).

REFERENCES

[1] On the promotion of electricity produced from renewable energy sources in the internal electricity market, Directive 2001/77/EC. [Online]. Available: http://eur-lex.europa.eu/
[2] M. Madrigal and S. Stoft, *Transmission Expansion for Renewable Energy Scale-Up: Emerging Lessons and Recommendations*. Washington, DC, USA: World Bank Publications, 2012.
[3] A. Liu *et al.*, "Co-optimization of transmission and other supply resources," Nat. Assoc. Regulatory Utility Commissioners, Washington, DC, USA, Rep. DE-OE0000316, 2013.
[4] F. D. Munoz, B. F. Hobbs, J. L. Ho, and S. Kasina, "An engineering-economic approach to transmission planning under market and regulatory uncertainties: WECC case study," *IEEE Trans. Power Syst.*, vol. 29, no. 1, pp. 307–317, Jan. 2014.
[5] E. E. Sauma and S. S. Oren, "Proactive planning and valuation of transmission investments in restructured electricity markets," *J. Regul. Econ.*, vol. 30, no. 3, pp. 261–290, 2006.
[6] F. D. Munoz, B. F. Hobbs, and S. Kasina, "Efficient proactive transmission planning to accommodate renewables," in *Proc. 2012 IEEE Power & Energy Soc. General Meeting*, Jul. 2012, pp. 1–7.
[7] A. H. van der Weijde and B. F. Hobbs, "The economics of planning electricity transmission to accommodate renewables: Using two-stage optimisation to evaluate flexibility and the cost of disregarding uncertainty," *Energy Econ.*, vol. 34, no. 6, pp. 2089–2101, 2012.
[8] J. H. Roh, M. Shahidehpour, and Y. Fu, "Market-based coordination of transmission and generation capacity planning," *IEEE Trans. Power Syst.*, vol. 22, no. 4, pp. 1406–1419, Nov. 2007.
[9] IRENA, "Renewable energy integration in power grids," Tech. Rep., 2015. [Online]. Available: http://www.irena.org/DocumentDownloads/Publications/IRENA-ETSAP_Tech_Brief_Power_Grid_Integration_2015.pdf
[10] NERC, "Potential reliability impacts of epa's clean power plan," Tech. Rep., 2015. [Online]. Available: http://www.nerc.com
[11] J. M. Morales, A. J. Conejo, and J. Perez-Ruiz, "Economic valuation of reserves in power systems with high penetration of wind power," *IEEE Trans. Power Syst.*, vol. 24, no. 2, pp. 900–910, May 2009.
[12] D. Pozo and J. Contreras, "A chance-constrained unit commitment with an n-K security criterion and significant wind generation," *IEEE Trans. Power Syst.*, vol. 28, no. 3, pp. 2842–2851, Aug. 2013.
[13] J. D. Lyon, K. W. Hedman, and M. Zhang, "Reserve requirements to efficiently manage intra-zonal congestion," *IEEE Trans. Power Syst.*, vol. 29, no. 1, pp. 251–258, Jan. 2014.
[14] Y. Chen, P. Gribik, and J. Gardner, "Incorporating post zonal reserve deployment transmission constraints into energy and ancillary service co-optimization," *IEEE Trans. Power Syst.*, vol. 29, no. 2, pp. 537–549, Mar. 2014.
[15] L. Bird, J. Cochran, and X. Wang, "Wind and solar energy curtailment: Experience and practices in the United States," Tech. Rep., Mar. 2014. [Online]. Available: http://www.nrel.gov/docs/fy14osti/60983.pdf
[16] NERC, "Transmission planning (TPL) standards." Web Page, 2016. [Online]. Available: http://www.nerc.com//

[17] A. Ben-Tal and A. Nemirovski, "Robust convex optimization," *Math. Oper. Res.*, vol. 23, no. 4, pp. 769–805, Nov. 1998.
[18] R. Jiang, J. Wang, and Y. Guan, "Robust unit commitment with wind power and pumped storage hydro," *IEEE Trans. Power Syst.*, vol. 27, no. 2, pp. 800–810, May 2012.
[19] D. Bertsimas, E. Litvinov, X. A. Sun, J. Zhao, and T. Zheng, "Adaptive robust optimization for the security constrained unit commitment problem," *IEEE Trans. Power Syst.*, vol. 28, no. 1, pp. 52–63, Feb. 2013.
[20] A. Moreira, A. Street, and J. M. Arroyo, "Energy and reserve scheduling under correlated nodal demand uncertainty: An adjustable robust optimization approach," in *Proc. 18th Power Syst. Comput. Conf.*, Wroclaw, Poland, Aug. 2014, pp. 1–8.
[21] R. A. Jabr, "Robust transmission network expansion planning with uncertain renewable generation and loads," *IEEE Trans. Power Syst.*, vol. 28, no. 4, pp. 4558–4567, Nov. 2013.
[22] C. Ruiz and A. Conejo, "Robust transmission expansion planning," *Eur. J. Oper. Res.*, vol. 242, no. 2, pp. 390–401, 2015.
[23] A. Moreira, A. Street, and J. M. Arroyo, "An adjustable robust optimization approach for contingency-constrained transmission expansion planning," *IEEE Trans. Power Syst.*, vol. 30, no. 4, pp. 2013–2022, Jul. 2015.
[24] Y. An and B. Zeng, "Exploring the modeling capacity of two-stage robust optimization: Variants of robust unit commitment model," *IEEE Trans. Power Syst.*, vol. 30, no. 1, pp. 109–122, Jan. 2015.
[25] S. Boyd and L. Vandenberghe, *Convex Optimization*. Cambridge, U.K.: Cambridge Univ. Press, 2004.
[26] C. Lee, C. Liu, S. Mehrotra, and M. Shahidehpour, "Modeling transmission line constraints in two-stage robust unit commitment problem," *IEEE Trans. Power Syst.*, vol. 29, no. 3, pp. 1221–1231, May 2014.
[27] Xpress Optimization Suite. [Online]. Available: http://www.fico.com/, Accessed in: Oct. 2016.
[28] A. Moreira, D. Pozo, A. Street, and E. Sauma. "Reliable renewable generation and transmission expansion planning–Case study input data," to be published. [Online]. Available: https://drive.google.com/drive/folders/0BxgJO6PuetvKOHRtNGtmMnZkUm8?usp=sharing
[29] CNE, "Fijación de precios de nudo, sistema interconectado central: Informe técnico definitivo," Rep., 2013. [Online]. Available: http://www.cne.cl/archivos_bajar/ITP_SIC_Abr04def.pdf
[30] CDEC-SIC, "Cálculo de peajes por el sistema de transmisión troncal," Web Page, 2013. [Online]. Available: http://www.cdec-sic.cl/
[31] MAPS Chile, "Mitigation options for addressing climate change," Web Page, 2015. [Online]. Available: http://mapschile.cl/
[32] R. Moreno, G. Strbac, F. Porrua, S. Mocarquer, and B. Bezerra, "Making room for the boom," *IEEE Power Energy Mag.*, vol. 8, no. 5, pp. 36–46, Sep. 2010.
[33] A. Papavasiliou, S. Oren, and B. Rountree, "Applying high performance computing to transmission-constrained stochastic unit commitment for renewable energy integration," *IEEE Trans. Power Syst.*, vol. 30, no. 3, pp. 1109–1120, May 2015.

Alexandre Moreira (S'12) received the degrees in electrical engineering and industrial engineering from the Pontifical Catholic University of Rio de Janeiro (PUC-Rio), Rio de Janeiro, Brazil, in 2011, and the M.Sc. degree from the Electrical Engineering Department, PUC-Rio, in 2014. He is currently working toward the Ph.D. degree in the Department of Electrical and Electronic Engineering, Imperial College London, London, U.K.

His current research interests include decision making under uncertainty as well as power system economics, operation, and planning.

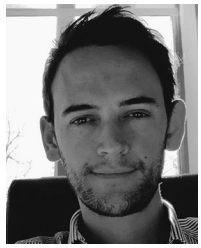

David Pozo (S'09–M'14) received the B.S. and Ph.D. degrees in electrical engineering from the University of Castilla-La Mancha, Ciudad Real, Spain, in 2006 and 2013, respectively. He is currently a Research Fellow in the Electrical Engineering Department, Pontifical Catholic University of Rio de Janeiro, Rio de Janeiro, Brazil. His research interests include power systems economics and electricity markets.

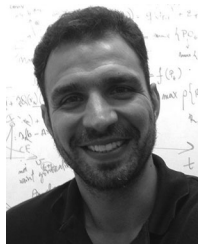

Alexandre Street (S'06–M'10) received the M.Sc. and D.Sc. degrees in electrical engineering (operations research) from the Pontifical Catholic University of Rio de Janeiro (PUC-Rio), Rio de Janeiro, Brazil.

In the beginning of 2008, he joined the Electrical Engineering Department, PUC-Rio, as an Assistant Professor to teach optimization. His research interests include power system economics, optimization methods, and decision making under uncertainty.

Enzo Sauma (M'06–SM'14) received the B.Sc. and M.Sc. degrees in electrical engineering from the Pontificia Universidad Catolica de Chile (PUC), Santiago, Chile, and the Ph.D. and M.Sc. degrees in industrial engineering and operations research from the University of California, Berkeley, CA, USA.

He is currently an Associate Professor in the Industrial and Systems Engineering Department, PUC. His research focuses on market-based transmission investment in restructured electricity systems.